

MESOSCALE STRUCTURE OF PRECIPITATION IN
EXTRATROPICAL CYCLONES

Peter V. Hobbs and Robert A. Houze, Jr.

University of Washington
Seattle, Washington

1. INTRODUCTION

Observational studies with radars, raingauges and aircraft consistently show that precipitation in extratropical cyclones is dominated by mesoscale rainbands which range in length from 100 to 1000 km and in width from 5 to 100 km (Harrold and Austin, 1974; Browning, 1974). In the CYCLES (Cyclonic Extratropical Storms) PROJECT at the University of Washington, we are investigating rainbands in extratropical cyclones, not only in terms of their morphology (which has been the emphasis of most previous studies), but also the physical processes associated with the bands. In this paper, we present examples of the rainbands which we have observed in occluded cyclones and suggest a classification scheme for them. The dynamics and microphysics of the clouds associated with rainbands will be illustrated by reference to a case study of an occluded frontal system.

2. TYPES OF RAINBANDS

We have observed six types of rainbands in the CYCLES PROJECT. These are illustrated in Fig. 1 and can be classified as follows:

Type 1: Warm frontal. Bands typically 50 km in width oriented parallel to warm front and found toward the leading edge of a frontal cloud shield (Band 1 in Fig. 1).

Type 2: Warm sector. Bands typically 50 km in width, found south of the intersection of the surface warm and cold fronts and tending to be parallel to cold fronts (Band 2 in Fig. 1).

Type 3: Cold frontal--wide. Bands approximately 50 km in width oriented parallel to cold front and found toward the trailing edge of a frontal cloud shield (Band 3 in Fig. 1).

Type 4: Cold frontal--narrow. An extremely narrow band (≈ 5 km in width) coinciding with the surface cold front (Band 4 in Fig. 1).

Type 5: Wave. Bands occurring in a very regular pattern similar to waves. Generally smaller than the other types of bands, typically 5 km \times 40 km, sometimes as large as 10 km \times 100 km (Bands labeled 5 in Fig. 1).

Type 6: Post frontal. Rainbands located in the convective cloud field behind a frontal cloud shield (Bands labeled 6 in Fig. 1).

The storm illustrated in Fig. 1 was somewhat unusual in exhibiting all six types of rainbands. While most of the storms which we have examined show some degree of banded structure, all types do not occur in every storm, nor do they occur in exactly the same arrangement in every case. However, when bands do appear, they are almost always one of the six types mentioned above.

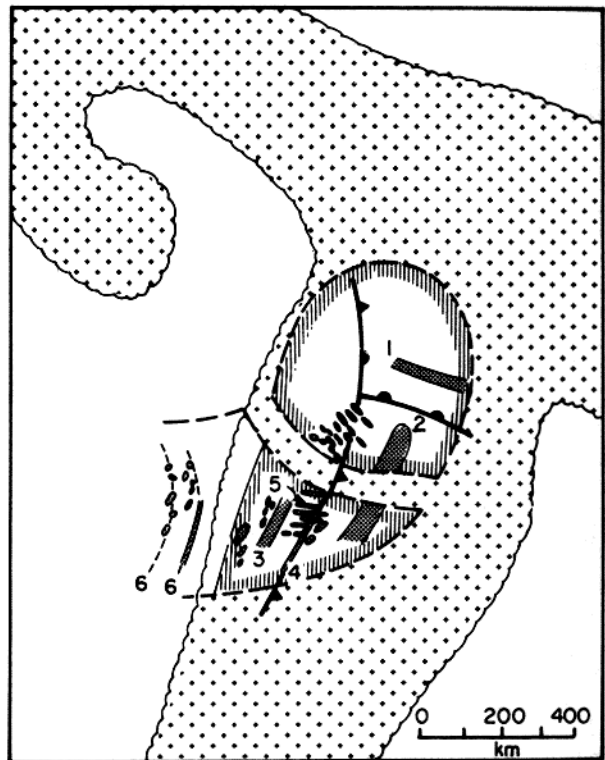


Fig. 1 Schematic presentation of occluded cyclone observed over the Pacific Northwest on 27-28 November 1973. Cloud pattern observed by satellite is shown by (*,*,*). Dashed lines enclose portion of cloud shield in which observations were obtained. Hatching (|||||) encloses light rain areas. Heavy rain areas are indicated by (|||||). Numbers refer to types of rainbands discussed in text.

Our classification scheme is consistent with rainbands observed in other parts of the world. Rainbands parallel to and ahead of warm fronts have been observed in open wave cyclones by Browning and Harrold (1969) and Reed (1972). These bands would be Type 1 in our classification. Browning and Harrold's observations were over the British Isles, while Reed's were in New England. Similar rainbands, with warm frontal orientation, were found in the leading (eastern) portions of occluded frontal systems described by Nagle and Serebreny (1962) over the eastern Pacific Ocean and by Kreitzberg and Brown (1970) over the northeastern U.S.

In the frontal systems studied by Nagle and Serebreny (1962) and Kreitzberg and Brown (1970), the Type 1 bands in the leading portion of the cloud shield gave way to bands with cold frontal orientations (which would be Type 2 by our classification) in the trailing western portion. In an occluded cyclone over the northeastern Atlantic Ocean, Browning *et al.* (1973) observed a series of Type 2 bands parallel to multiple cold fronts aloft. Their Type 2 bands, however, were apparently not preceded by a series of warm frontal bands.

Warm sector bands (Type 3 in our classification) were observed frequently in open wave cyclones near Japan by Nozumi and Arakawa (1968). They found that the warm sector bands tended to be parallel to the cold front, often intersection the warm front at right angles. Harrold (1973) also reported that warm sector bands parallel to the cold front occurred frequently in cyclones near the British Isles. Browning and Harrold (1969) found warm-sector rainbands over England which were not parallel to either the cold or warm front in a wave depression; however, the orientation of these bands may have been influenced by the topography of the British Isles. The pre-frontal squall line associated with severe convective storms is a notable special case of Type 3 (warm sector) rainbands.

Type 4 rainbands, that is, long, thin and continuous rainbands coinciding with surface cold fronts, have been observed previously by Kessler and Wexler (1960) in New England and by Browning and Pardoe (1973) in six cases over the British Isles.

Post-frontal convective rainbands (Type 6) were included by Nagle and Serebreny (1962) in their schematic model of radar echoes in occluded cyclones over the eastern Pacific Ocean. The occurrence of mesoscale precipitation bands in cold air masses to the west of surface cyclonic systems is a well known phenomenon during the winter over the Sea of Japan (e.g., Matsumoto *et al.*, 1967).

3. RAINBANDS IN RELATION TO FRONTAL AIR MOTIONS

Besides the morphology of the rainbands, evident in raingauge and radar data, we are employing the CYCLES PROJECT data to investigate the dynamics and microphysics of the

clouds associated with the bands. For illustration, we refer to the storm depicted in Fig. 2, which was an occluded frontal system containing

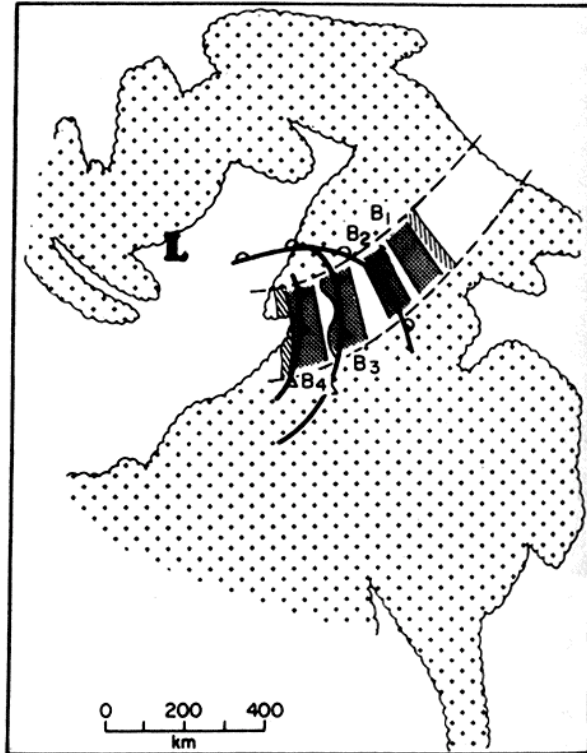


Fig. 2 Schematic representation of storm observed over Washington State on 20 December 1973. Cloud pattern observed by satellite is shown by (*+*+*). Dashed lines enclose portion of cloud shield in which observations were obtained. Hatching (|||||) encloses light rain areas. Rainbands are denoted B₁-B₄. Fronts shown are for 720 mb level.

two Type 1 (warm frontal) rainbands (B₁ and B₂ in Fig. 2) and two Type 3 (cold frontal-wide) rainbands (B₃ and B₄ in Fig. 2).

The dynamical framework in which the rainbands existed is illustrated by Figs. 3 and 4. The two-dimensional vertical circulation pattern shown in Fig. 3 was obtained by subtracting the horizontal velocity of the frontal system from the winds observed with serial rawinsondes; it therefore represents the airflow relative to the system. Vertical velocities were computed using the two-dimensionalized mass continuity equation in the plane of the cross section.

The computed flow pattern in Fig. 3 is in good agreement with other data. The region of maximum upward motion in the lower troposphere is centered on the time of the surface trough passage (T in Fig. 3), when the maximum low-level convergence would be expected. The computed upward motion region also coincides exactly with the periods of precipitation and satellite-observed cloudiness at the rawinsonde site. The airflow pattern shown in Fig. 3 is remarkably similar to frontal airflow patterns obtained in previous investigations of Pacific occlusions (Elliott and Hovind, 1965; Hobbs *et al.*, 1975).

The flow of water vapor through the region of upward motion (enclosed by the dashed line in Fig. 3) shows that the primary

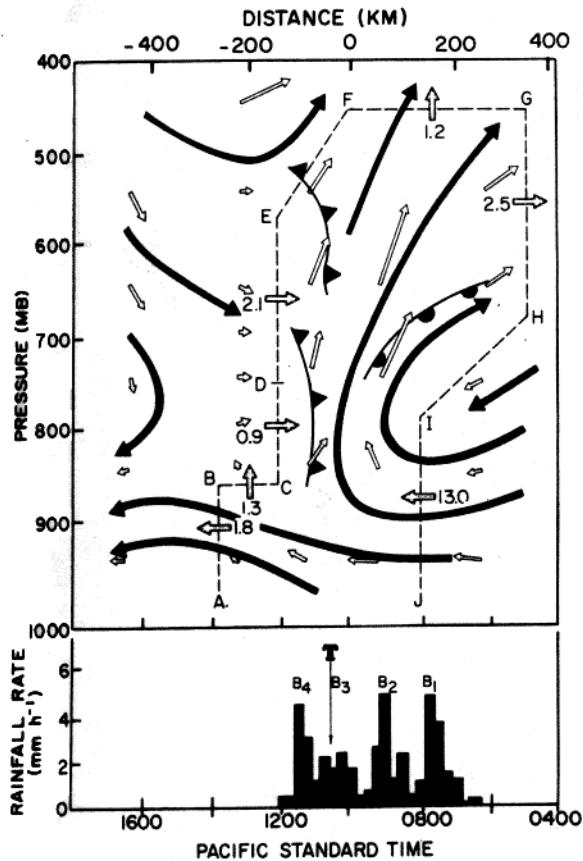


Fig. 3 Two-dimensional airflow in the frontal system of 20 December 1973. Distance scale at top of diagram was obtained by converting time to space on the basis of observed frontal velocities. Streamlines relative to fronts are shown by heavy arrows (→). Small open arrows (⇨) indicate the displacement of a parcel of air in one hour at the computed velocity applying at its origin (vertical component in mb, horizontal component in km). Dashed line surrounds region of upward motion associated with frontal clouds and rainbands (B₁-B₄). Striped arrows crossing dashed line show fluxes of water vapor (with numbers adjacent to arrows indicating magnitudes of fluxes in units of 10⁴ g s⁻¹ m⁻¹) across boundaries of lifting region. Letters A-J mark points referred to in text. Letter T marks time of surface trough passage.

source of moisture for the region containing the rainbands was the low-level flow through the boundary IJ below the warm front.

The origin of the moist air feeding rainbands B₁-B₄ was investigated by estimating the three-dimensional trajectories of the air flowing through the cross section of Fig. 3. We identified four air parcels in the cross section plane and displaced them backwards in time (in one-hour steps) according to the computed vertical velocity field shown in Fig. 3 and the observed horizontal winds. It was assumed that the airflow in the plane of the cross section of Fig. 3 applied everywhere along

a 600 km length of the frontal system. The computed trajectories are shown in Fig. 4. In Fig. 4(a), the frontal motion has been subtracted from the trajectories to show the flow relative to the fronts, while in Fig. 4(b), the trajectories are shown relative to the earth.

From the geographical frame of reference in Fig. 4(b), it is evident that the moisture influx along trajectories W, X, and Y originated from the south to south-southwest of the lifting zone with the moist air moving toward the front in a relative sense at low levels and beginning to rise only as it was overtaken by the approaching frontal system. This trajectory pattern is very similar to that observed by Hobbs et al. (1975) who further showed how such an airflow can be disrupted as it moves over a north-south oriented mountain range.

4. SMALL MESOSCALE AREAS WITHIN RAINBANDS

The mesoscale rainbands in extratropical cyclones typically contain a pattern of small mesoscale (~10 km in horizontal dimension) and cumulus-scale (~1 km in horizontal dimension) cores of heavy rainfall (Austin and Houze, 1972). Figure 5 shows the track of a typical small mesoscale area which was located in band B₁. This small rain area passed over the University of Washington (UW) radar site during "period 2" of the (UW) raingauge trace seen in Fig. 6. It is seen that the rain during period 2 was generally enhanced and consisted of several peaks of heavy rainfall, each 1 to 3 min in duration, suggesting that the small mesoscale rain area contained cumulus-scale convection.

Figure 6 contains a time cross-section of vertically-pointing pulsed Doppler radar data showing the mean fall speeds of precipitation particles averaged over 3 min periods in band B₁. Since the radar data in Fig. 6 were averaged over 3 min periods, they probably do not fully resolve the embedded convection during period 2; however, the radar data for period 2 do show relatively short periods of enhanced fall speeds which were not present before or after period 2. This is especially notable above the melting layer, where the velocity field was uniform during period 1 but quite variable during period 2.

Serial rawinsonde data collected during the passage of band B₁ showed that the air between 4 and 5 km altitude was potentially unstable and was being brought to saturation by the lifting over the warm front portrayed in Fig. 3. The instability released in the 4-5 km layer aloft apparently accounted for the convective structure seen in the precipitation at lower levels during period 2 of Fig. 6.

5. CLOUD MICROSTRUCTURE ASSOCIATED WITH RAINBANDS

Weiss and Hobbs (1974) have shown that ice particle growth modes can be related to the vertical gradient of the mean particle fall speed. A small gradient ($\leq 10^{-4}$ s⁻¹ in magnitude) is associated with growth by deposition from the vapor phase while larger gradients

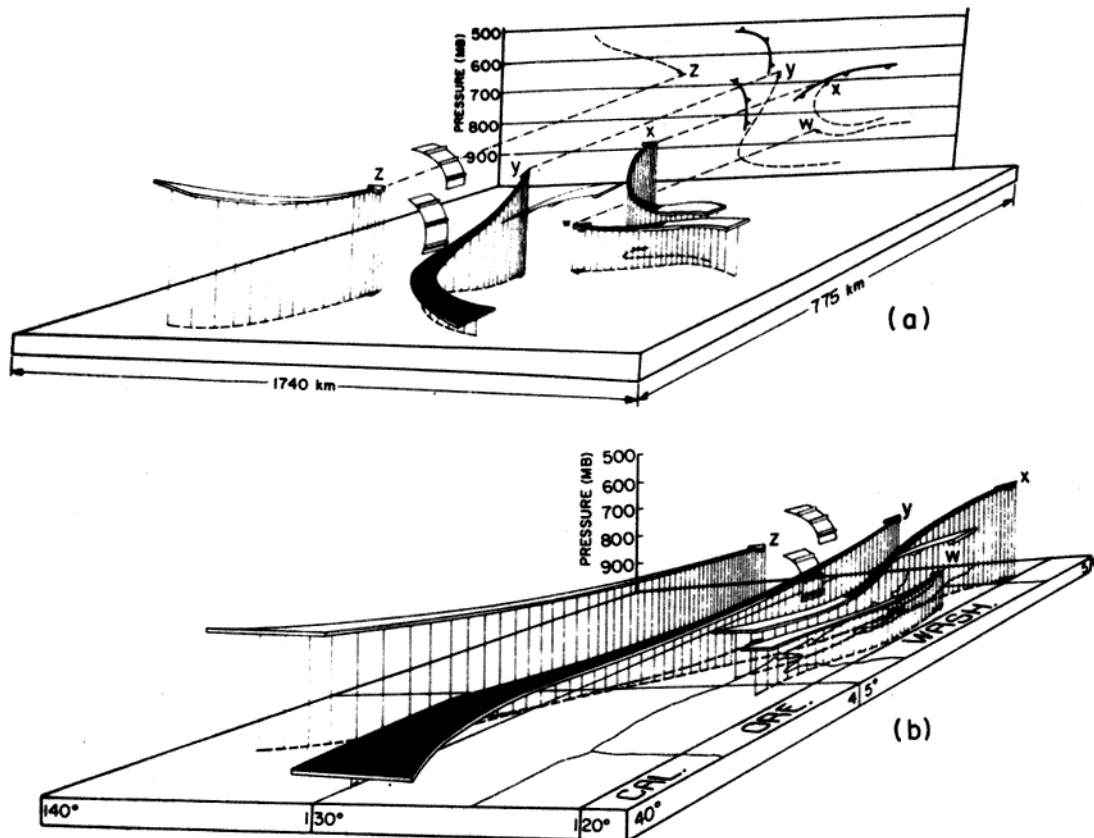


Fig. 4 Three-dimensional trajectories for frontal system of 20 December 1973. Trajectories are for a seven-hour period. In (a) trajectories are shown relative to fronts, while in (b) they are shown relative to the Earth. The background of (a) shows the two-dimensional projections of trajectories W, X, Y and Z in a format similar to that of Fig. 3. Upward moving portions of trajectories are shaded black.

are associated with growth by collection processes (either riming or aggregation). Applying these ideas to Fig. 6, we conclude that the region above about 2.8 km, which was characterized primarily by a very small vertical gradient of fall speed, was dominated by depositional growth. Just below 2.8 km, but above the top of the melting layer, the isotachs of fall speed in Fig. 6 are horizontally oriented and the larger vertical gradient of fall speed ($\sim 10^{-3} \text{ s}^{-1}$) indicates that the particles were growing by riming or aggregation in this region.

The cloud microstructure deduced from the Doppler radar was confirmed by direct aircraft sampling (Fig. 7). Ice particles were sampled aboard the University of Washington B-23 research aircraft which flew within the "collectional growth region" deduced from the Doppler radar (Fig. 6). Growth by collectional processes was indicated directly by Formvar and metal foil replication data which showed visual evidence of ice particle aggregation, and the in-cloud temperature, liquid water content, droplet sizes and ice particles sizes which appeared to be favorable for riming.

Ice concentrations measured on board the aircraft in rainbands B₃ and B₄ (Fig. 7) were in the range of 10-200 l^{-1} . This value exceeds the active cloud nucleus concentration to be expected at a cloud top temperature of

-14°C (estimated from rawinsonde data) by a factor of $10^{1.5}$ to $10^{3.8}$, indicating that ice enhancement was probably occurring in the rainbands. The ice enhancement could have been produced by ice multiplication during riming, since the conditions at flight level were similar to those which Mossop (1976) observed to produce ice splinters in laboratory experiments.

6. CONCLUDING REMARKS

Morphological studies of rainfall patterns have shown that there are six types of mesoscale rainbands which tend to occur in extratropical cyclones. We have observed these six types of rainbands in extratropical storms in the Pacific Northwest, and comparison with studies of mid-latitude cyclones conducted in other parts of the world indicates that these rainband types occur rather generally in extratropical cyclones.

The dynamics and microphysics of the cloud systems producing the rainbands can be investigated effectively by making simultaneous and well-coordinated rawinsonde, radar, raingauge and aircraft measurements in cyclonic storms. Data collected in this way cover scales ranging from the synoptic scale down to cloud particle scales and permit an examination of both the physical framework within which the rainbands exist and the processes which are at work within them.

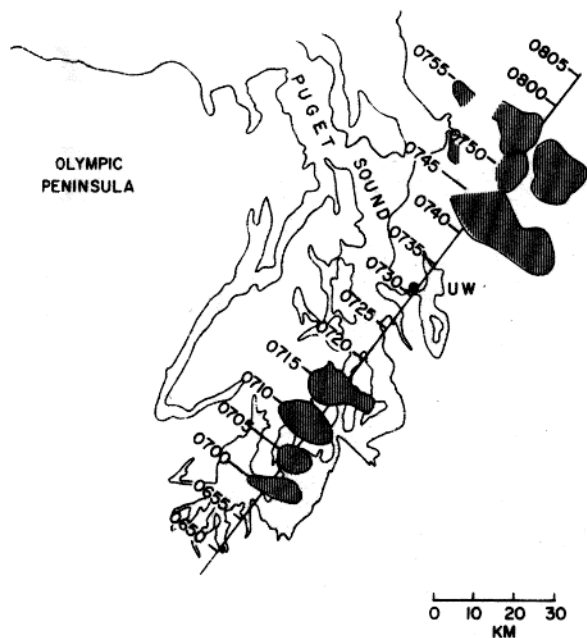


Fig. 5 Path of small mesoscale rain echo (darkest shading) seen on University of Washington (UW) radar PPI on 20 December 1973. Times of interpolated echo positions are shown in the immediate vicinity of UW where the rain echo was obscured by ground clutter echoes.

In a case study from the CYCLES PROJECT, air motions inferred from serial rawinsonde data showed that the rainbands in an occluded frontal system were supplied with moisture flowing into the rainband region from the south to south-southwest at low levels (below 800 mb). This air was swept abruptly upward in the rainbands just ahead of the cold air mass approaching from the west. A small mesoscale area of heavy rain within one of the rainbands in this storm was found to contain cells of cumulus-scale dimension which apparently resulted from the release of potential instability by lifting above the warm front. Vertically-pointing Doppler radar measurements indicated that as ice particles settled below the layer containing the convective cells, they grew first by vapor deposition and then, just above the melting layer, by riming or aggregation. Direct aircraft sampling of ice particles in the rainbands confirmed results inferred from the radar data. Aircraft measurements of ice particle concentrations indicated that ice enhancement was occurring in the clouds associated with the rainbands.

Case studies such as the one described here can be improved greatly by multi-level aircraft sampling in the rainbands. Particle growth modes deduced from radar data can then be checked more effectively by direct particle sampling than is possible with aircraft data from a single level. Weather radars can be used in real time to identify and

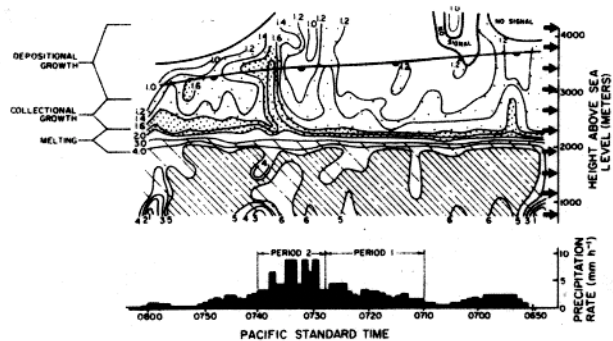


Fig. 6 Vertical cross section showing contours of three-minute average precipitation fall speeds ($m s^{-1}$) measured with Doppler radar during the passage of rainband B₁. High resolution rainfall trace obtained at the radar site is also shown.

monitor the rainbands and direct the research aircraft into different levels in the bands. Studies of this type are now underway as part of the CYCLES PROJECT.

ACKNOWLEDGMENT

This research was supported by the Atmospheric Research Section (Meteorology Program) of the National Science Foundation (Grant ATM74-14726-A02) and by Contract No. F19 628-74-C-0066 from Air Force Cambridge Research Laboratories.

REFERENCES

- Austin, P.M. and R.A. Houze, Jr., 1972: Analysis of the structure of precipitation patterns in New England. *J. Appl. Meteor.*, **11**, 926-935.
- Browning, K.A., 1974: Mesoscale structure of rain systems in the British Isles. *J. Meteor. Soc. Japan*, **50**, 314-327.
- _____, and T.W. Harrold, 1969: Air motion and precipitation growth in a wave depression. *Quart. J. Roy. Meteor. Soc.*, **95**, 288-309.
- _____, and C.W. Pardoe, 1973: Structure of low level jet streams ahead of mid-latitude cold fronts. *Quart. J. Roy. Meteor. Soc.*, **99**, 619-638.
- _____, M.E. Hardman, T.W. Harrold, and C.W. Pardoe, 1973: The structure of rainbands within a mid-latitude depression. *Quart. J. Roy. Meteor. Soc.*, **99**, 215-231.
- Elliott, R.D., and E.L. Hovind, 1965: Heat, water and vorticity balance in frontal zones. *J. Appl. Meteor.*, **4**, 196-211.
- Harrold, T.W., 1973: Mechanisms influencing the distribution of precipitation within baroclinic disturbances. *Quart. J. Roy. Meteor. Soc.*, **99**, 232-251.
- _____, and P.M. Austin, 1974: The structure of precipitation systems - a review. *J. de Rech. Atmosph.*, **8**, 41-57.

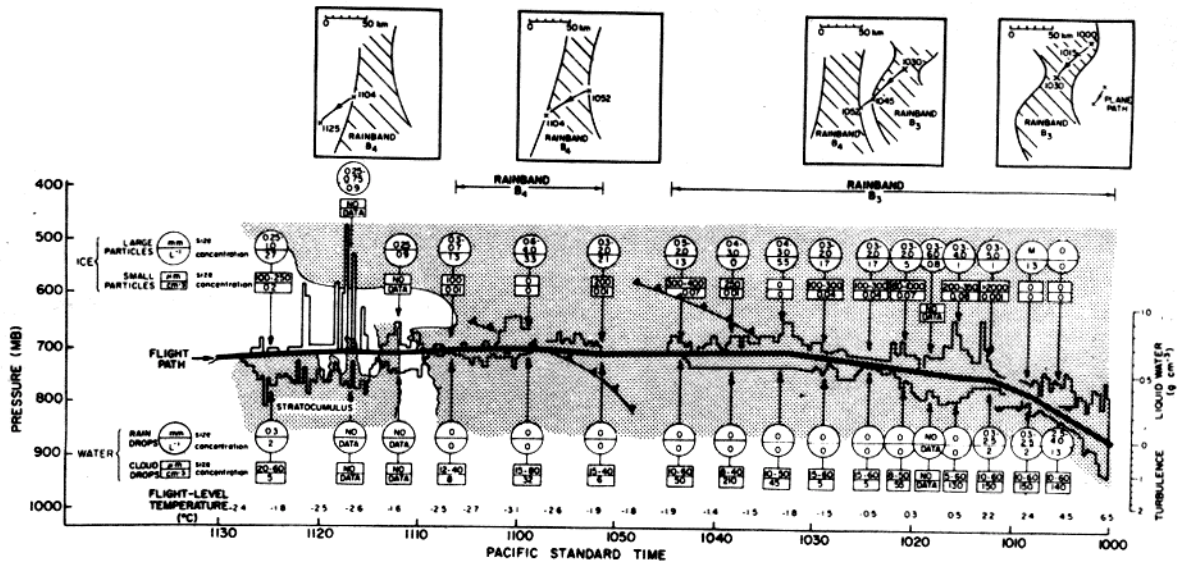


Fig. 7 Vertical cross sections showing aircraft measurements obtained in clouds associated with rainbands B₃ and B₄. The inset drawings show plan views of the aircraft's flight path in relation to rainbands. In the vertical cross section, shaded areas indicate cloudy regions. The origins of the turbulence and liquid water content plots are centered on the flight path line. Whereas, turbulence and liquid water content were measured continually during the flight, ice particle and drop sizes and concentrations (indicated in circles and boxes) were determined only at discrete intervals by replication sampling. The letter M indicates particles were melting and therefore could not be accurately sized.

Hobbs, P.V., R.A. Houze, Jr., and T.J. Matejka, 1975: The dynamical and microphysical structure of an occluded frontal system and its modification by orography. J. Atmos. Sci., 32, 1542-1562.

Kessler, E., and R. Wexler, 1960: Observations of a cold front, 1 October 1958. Bull. Amer. Meteor. Soc., 41, 253-257.

Kreitzberg, C.W., and H.A. Brown, 1970: Mesoscale weather systems within an occlusion. J. Appl. Meteor., 9, 417-432.

Matsumoto, S., K. Ninomiya, and T. Akiyama, 1967: A synoptic and dynamic study on the three-dimensional structure of mesoscale disturbances observed in the vicinity of a cold vortex center. J. Met. Soc. Japan, 45, 64-81.

Mossop, S.C., 1976: Production of secondary ice particles during the growth of graupel by riming. Quart. J. Roy. Meteor. Soc., 102, 45-56.

Nagle, R.E., and S.M. Serebreny, 1962: Radar precipitation echo and satellite observations of a maritime cyclone. J. Appl. Meteor., 1, 279-295.

Nozumi, Y., and H. Arakawa, 1968: Prefrontal rainbands located in the warm sector of subtropical cyclones over the ocean. J. Geophys. Res., 78, 487-492.

Reed, R.W., 1972: Characteristics and development of mesoscale precipitation areas in extratropical cyclones. S.M. Thesis, Dept. of Meteorology, Massachusetts Institute of Technology, 94 pp.

Weiss, R.R., and P.V. Hobbs, 1975: The use of a vertically pointing pulsed Doppler radar in cloud physics and weather modification studies. J. Appl. Meteor., 14, 222-231.